Acta Cryst. (1998). D**54**, 1359–1366

Static Laue Diffraction Studies on Acetylcholinesterase

Raimond B. G. Ravelli,[a]† Mia L. Raves,[b]† Zhong Ren,[c] Dominique Bourgeois,[d] Michel Roth,[d] Jan Kroon,[a] Israel Silman[e] and Joel L. Sussman[b,f]*

[a]*Department of Crystal and Structural Chemistry, Bijvoet Center for Biomolecular Research, Utrecht University, Padualaan 8, 3584 CH Utrecht, The Netherlands,* [b]*Department of Structural Biology, Weizmann Institute of Science, 76100 Rehovot, Israel,* [c]*Department of Biochemistry and Molecular Biology, The University of Chicago, 920 East 58th Street, Chicago, IL 60637, USA,* [d]*Institut de Biologie Structurale Jean-Pierre Ebel, 41 Avenue des Martyrs, 38027 Grenoble CEDEX 1, France,* [e]*Department of Neurobiology, Weizmann Institute of Science, 76100 Rehovot, Israel, and* [f]*Biology Department, Brookhaven National Laboratory, Upton NY 11973-5000, USA.*
E-mail: joel.sussman@weizmann.ac.il

(*Received 16 October 1997; accepted 6 April 1998*)

Abstract

Acetylcholinesterase (AChE) is one of nature's fastest enzymes, despite the fact that its three-dimensional structure reveals its active site to be deeply sequestered within the molecule. This raises questions with respect to traffic of substrate to, and products from, the active site, which may be investigated by time-resolved crystallography. In order to address one aspect of the feasibility of performing time-resolved studies on AChE, a data set has been collected using the Laue technique on a trigonal crystal of *Torpedo californica* AChE soaked with the reversible inhibitor edrophonium, using a total X-ray exposure time of 24 ms. Electron-density maps obtained from the Laue data, which are of surprisingly good quality compared with similar maps from monochromatic data, show essentially the same features. They clearly reveal the bound ligand, as well as a structural change in the conformation of the active-site Ser200 induced upon binding.

1. Introduction

1.1. *Reaction of AChE*

The principal function of the enzyme acetylcholinesterase (AChE; E.C. 3.1.1.7) is rapid hydrolysis of the neurotransmitter acetylcholine (ACh) in the central nervous system and at vertebrate neuromuscular junctions (Massoulié *et al.*, 1993). As demanded by this biological role, it is an extremely efficient catalyst, approaching a reaction velocity at which substrate diffusion becomes rate limiting, with a turnover number of $\sim$20000 s^{-1} (Quinn, 1987). The X-ray structure of *T. californica* AChE (*Tc*AChE) (Sussman *et al.*, 1991) unexpectedly revealed that the active-site residues are buried within the protein, apparently accessible only *via* a long and narrow gorge lined with aromatic residues. The AChE molecule displays an asymmetric charge distribution, resulting in a strong dipole moment aligned approximately along the active-site gorge (Ripoll *et al.*, 1993; Tan *et al.*, 1993). It has been suggested that the electric field so generated attracts the positively charged ACh to the rim of the gorge (Ripoll *et al.*, 1993). The substrate is then guided by the electric field, using the aromatic residues in the gorge as a series of low-affinity sites, towards the active site. The side chains of two aromatic residues, Trp84 and Phe330, serve as the so-called anionic site for binding the quarternary moiety of ACh *via* cation–π interactions (Verdonk *et al.*, 1993; Dougherty, 1996). Hydrolysis of ACh to choline and acetate is accomplished by the catalytic triad consisting of Ser200, His440 and Glu327, with Ser200 being transiently acetylated (Quinn, 1987).

The narrow dimensions of the active-site gorge, together with the potential gradient along it, raise cogent questions regarding the traffic of substrate and products to and from the active site. Thus, in addition to steric considerations, the potential along the gorge would be expected to accelerate expulsion of acetate but retard release of choline from the active site. Furthermore, movement of water between the bulk phase and the gorge must be taken into account. Theoretical calculations, however, showed that it is still possible for choline to go back through the gorge sufficiently rapidly if there is no steric hindrance (S. Lifson, S. Botti and C. Felder, personal communications). A second possibility that has been proposed (Ripoll *et al.*, 1993) is that choline leaves through a back door – a transient opening in the thin aspect of the gorge wall arising by movement of one or more residues (Gilson *et al.*, 1994). The residues that contribute to the opening of the putative back door are expected to be located on the Ω-loop between Cys67 and Cys94 in *Tc*AChE (Axelsen *et al.*, 1994), a loop which is known to adopt an open and closed conformation in the structurally similar enzyme *Candida rugosa* lipase (Grochulski *et al.*, 1994). Further evidence

† Both authors contributed equally to this work.

for an alternative entrance to the gorge comes from studies on the mode of inhibition of AChE by the potent snake-venom polypeptide toxin, fasciculin. Crystallographic studies clearly demonstrate that the toxin completely blocks the entrance to the active-site gorge (Bourne *et al.*, 1995; Harel *et al.*, 1995). Nevertheless, significant residual catalytic activity can be observed in solution (Marchot *et al.*, 1993). Site-directed mutagenesis studies which were designed to prove the importance of the mobility of certain residues did not, however, provide support for the existence of a back door (Kronman *et al.*, 1994; Faerman *et al.*, 1996).

1.2. *Laue method*

Time-resolved crystallography is clearly an approach with the potential to provide direct experimental information to either support or refute the existence of a back door, and the Laue diffraction method has been employed successfully in recent years to observe enzyme reactions as they occur in the crystal state (Schlichting *et al.*, 1990; Bolduc *et al.*, 1995). The technique is attractive due to the very short exposure times required. Recently, crystallographic snapshots have been reported of structural changes occurring in a protein on a time scale as short as nanoseconds (Šrajer *et al.*, 1996). A prerequisite for successful Laue measurements is the achievement of a high degree of synchronization of the initiation of the reaction. In some cases, the substrate is immobilized by attachment of a photosensitive chemical moiety, effectively turning it into an inhibitor. Such caged compounds can then be activated by photolysis, usually with laser flashes. In the case of AChE, a series of caged compounds, which generate either choline or carbamylcholine (CCh) upon photolysis (Peng & Goeldner, 1996; Peng *et al.*, 1996), have been synthesized and characterized photochemically and enzymatically. CCh is a substrate of AChE; the first step of the reaction, carbamylation of the enzyme, is rapid, but decarbamylation is slow, on a time scale of minutes at room temperature (Wilson *et al.*, 1960). It is envisaged that synchronized photolysis of caged CCh within the crystal will produce rapid release of choline by the enzymatic machinery and that movement of choline and concomitant changes in the protein conformation may be monitored by the Laue method.

The Laue technique has some inherent difficulties, such as a paucity of low-resolution reflections, overlap of multiple spots, spatial overlap of streaked spots and an unfavourable peak-to-background ratio (Hajdu *et al.*, 1991). These drawbacks result in a requirement for well diffracting crystals with low mosaic spread. Since success in Laue diffraction experiments is not guaranteed even if good diffraction is obtained under conditions of a monochromatic experiment, we decided to evaluate the quality of the data obtainable by the Laue technique for trigonal crystals of *Tc*AChE (Sussman *et al.*, 1991). Our initial goal was to obtain a data set of sufficient quality to permit the resolution of structural features within the active site of the enzyme. To test this, crystals were soaked with a solution of a small ligand, edrophonium [ethyl(3-hydroxyphenyl)dimethyl ammonium, see Fig. 1] which is a known reversible inhibitor of AChE. The structure of the complex of *Tc*AChE with edrophonium was determined earlier using monochromatic radiation (Harel *et al.*, 1993). Comparison of electron-density maps obtained from Laue data with maps obtained from monochromatic data should reveal whether use of the Laue technique is feasible for performing time-resolved studies on AChE.

2. Methods and results

2.1. *Monochromatic reference data*

A monochromatic data set on the AChE–edrophonium complex was collected as a reference to provide a fair comparison with the Laue data set. The new data set was obtained from crystals grown in the same way as those for the Laue data set, using PEG 200 as a precipitant (Raves *et al.*, 1997), whereas the crystals used to obtain the previously reported AChE–edrophonium data (Harel *et al.*, 1993) were grown from ammonium sulfate. In order to obtain data of the highest possible quality, the new data set was collected at a synchrotron source (EMBL outstation of the DESY in Hamburg, Germany, beamline X11, λ = 0.92 Å, 30 cm MAR Research image-plate detector). The crystal, 0.3 × 0.3 × 0.2 mm, was cooled to 277 K and had a mosaic spread of 0.29°. It diffracted to a resolution of 2.4 Å; further details on the quality of this data set are given in Table 1. The structure obtained from the monochromatic synchrotron data set is virtually identical to the previously determined structure with PDB access code 1ACK (Harel *et al.*, 1993); the r.m.s. deviation between coordinates for all Cα atoms is 0.29 Å, and a plot of the r.m.s. deviations of the backbone *versus* the residue number does not show any major conformational

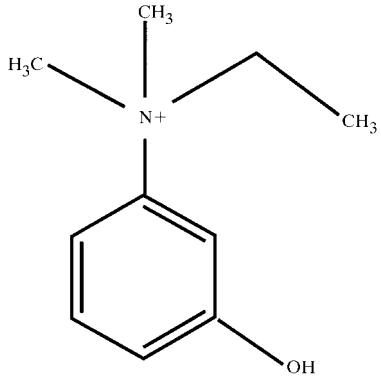

Fig. 1. Structural diagram of edrophonium.

Table 1. *Monochromatic diffraction data statistics*

Number of frames	66
Oscillation angle (°)	0.75
Cell parameters ($P3_121$) (Å)	$a = b = 112.41$, $c = 136.55$
Mosaicity (°)	0.29
Number of observations	275832
Unique reflections	38611
Overall redundancy	3.1
Highest resolution shell†	3.1
R_{sym} (%)‡	8.9
Highest resolution shell†	42.0
Average I/σ	14.0
Highest resolution shell†	2.1
Completeness (%)	97.7
Highest resolution shell†	99.6

† Highest resolution shell: 2.46–2.40 Å. ‡ $\sum_h \sum_i |I_{h_i} - \langle I_h \rangle| / \sum_h \sum_i I_{h_i}$.

changes. The r.m.s. deviation for the 12 non-H atoms of the ligand is 0.30 Å.

2.2. *Laue data collection*

Laue data on crystals of AChE soaked with edrophonium were collected at the European Synchrotron Radiation Facility (ESRF) in Grenoble, France, at the white-radiation beamline BL3 (ID9), with a wavelength range of 0.4–1.5 Å. With the synchrotron operating in 1/3 fill mode at 200 mA, the crystals, mounted in a capillary, were tested at a temperature of 277 K using an FTS cooling device. Several crystals had to be discarded due to lack of high-resolution reflections and/or severe streaking of the spots. Good diffraction was obtained from a rather large crystal, 0.5 × 0.5 × 0.4 mm, that showed a reasonably low mosaicity. 24 still frames with an exposure time of 1 ms each and a crystal-to-film distance of 300 mm were collected while rotating the crystal over 5° along the spindle axis between exposures. The data, collected on an X-ray image intensifier coupled to a CCD camera, were corrected for spatial distortions and non-uniformity of response with the package *fit2d* (Hammersley *et al.*, 1994).

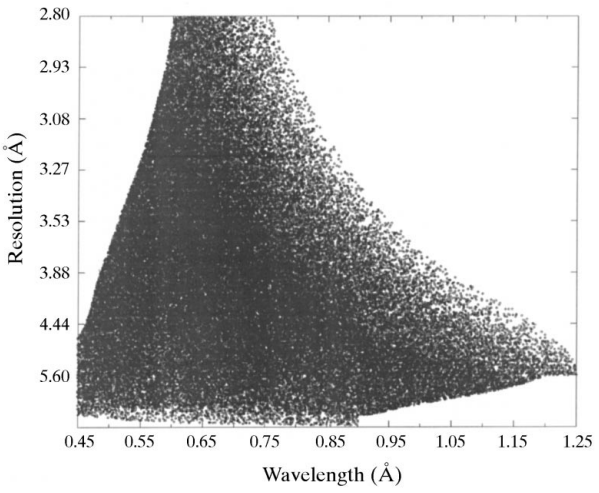

Fig. 2. Distribution of single reflections: resolution *versus* wavelength. The Bragg angle cut-off is clearly seen at higher wavelengths and higher resolution (see Ren & Moffat, 1995*a*).

2.3. *Laue data processing*

The crystal-orientation parameters and relative cell dimensions were determined using the program *LaueCell* (Ravelli *et al.*, 1996). The scaled cell dimensions ($a = b = 113.0$, $c = 136.8$ Å) are close to the values found for monochromatic data on non-frozen trigonal *Tc*AChE crystals in general. The program *LaueView* (Ren & Moffat, 1995*a*) was used for further processing of the data. The Laue spots on the patterns were predicted using a resolution-dependent wavelength bandpass, based on a known starting λ-curve and Wilson statistics. The wavelength normalization was performed in two parts, since the distribution of the single spots as a function of the wavelength is not uniform (see Fig. 2); the single spots are densely distributed between 0.45 Å (λ_{min}) and 0.9 Å ($2\lambda_{min}$) and relatively sparsely at wavelengths higher than $2\lambda_{min}$. The λ-curve for wavelengths between 0.45 and 0.9 Å was simulated with a 16-term Chebyshev polynomial and the curve for wavelengths between 0.9 and 1.25 Å with a three-term Chebyshev. Fig. 2 also shows a Bragg-angle cut-off (*i.e.* no spots in the upper right-hand corner of the figure); the crystal diffracted beyond the edge of the detector. The risk of overlapping spots, however, prevented a significant reduction of the crystal-to-detector distance. The resolution limit (d_{min}) used for the processing of the Laue data set is 2.8 Å, compared with 2.4 Å for the monochromatic data. The combined λ-curve (shown in Fig. 3) was used for deconvolution of the multiples (Ren & Moffat, 1995*b*), which significantly increased the completeness of the data, especially in the ∞–$2d_{min}$ range. Details of the quality of the Laue data set are given in Table 2. The overall completeness is 84.5%. The amplitudes of the full Laue data set give a correlation of 91.6% with those of corresponding reflections in the monochromatic data set (see Fig. 4); for the singles, the correlation is 93.4% and for the deconvoluted multiples, 87.8%.

2.4. *Refinement*

The same refinement procedure was used for both the monochromatic and the Laue data set. The coordinates of native *Tc*AChE in the trigonal crystal form (PDB access code 2ACE; Raves *et al.*, 1997) were used as a starting model; 5% of the data (1891 reflections for the monochromatic, 1032 for the Laue data) were reserved in a test set for cross-validation of the refinement process. To reduce the chance of introducing model bias into the initial maps, the reflections for the test set were taken by selecting the corresponding reflections from

Table 2. *Laue diffraction data statistics*

Number of frames	24
Exposure time (ms)	1
Cell parameters ($P3_121$) (Å)	$a = b = 113.00$, $c = 136.80$
Singles	
Number of observations†	83171
Unique reflections	19613
Overall redundancy	4.2
R_{sym} (%)‡	
Unweighted	14.8
Weighted	10.8
Singles and multiples combined	
Number of deconvoluted multiples	5464
Total number of unique reflections	21122

Resolution (Å)	Completeness (%)§		R_{sym} (%)‡
	Shell	Cumulative	
∞–11.2	42.0	42.0	14.7
11.2–8.4	77.6	62.7	13.0
8.4–5.6	91.2	82.8	12.8
5.6–4.0	95.1	90.6	13.5
4.0–3.4	95.3	92.4	15.2
3.4–3.0	87.3	90.4	21.3
3.0–2.8	61.3	84.5	25.0

† After rejection of weak spots and those with negative intensity $[I/\sigma(I) < 0.1]$, high background, bad profile fitting and/or bad merging $[|F^2_{\mathbf{h}_i} - \langle F^2_{\mathbf{h}}\rangle|/\sigma(\langle F^2_{\mathbf{h}}\rangle) > 15]$. ‡ $R_{sym} = \sum_{\mathbf{h}}\sum_i(w_{\mathbf{h}_i}|F^2_{\mathbf{h}_i} - \langle F^2_{\mathbf{h}}\rangle|)/\sum_{\mathbf{h}}\sum_i w_{\mathbf{h}_i}F^2_{\mathbf{h}_i}$, where $\langle F^2_{\mathbf{h}}\rangle = \sum_i w_{\mathbf{h}_i}F^2_{\mathbf{h}_i}\sum_i w_{\mathbf{h}_i}$ and $w_{\mathbf{h}_i} = 1/\sigma^2(F^2_{\mathbf{h}_i})$ for weighted R factor and $w_{\mathbf{h}_i} = 1$ for unweighted R factor. § Completeness by resolution shell for singles and multiples combined. Binning is partly based on d_{min} value (2.8 Å): $4d_{min}$, $3d_{min}$, $2d_{min}$ and equal shell volume for resolutions higher than $2d_{min}$.

the test set used for refinement of the native structure. Initial maps were calculated after rigid-body movement of the coordinates for protein residues of the native AChE structure using the program *X-PLOR* Version 3.851 (Brünger *et al.*, 1987). The difference between R and R_{free} at this point was 2.6% for the monochromatic and 2.2% for the Laue data, compared to 3.6% for the final stage of refinement of 2ACE without water. A random test set would have given R and R_{free} of the same value; the differences obtained indicate that most of the model bias has been avoided. Subsequent refinement was performed using the maximum-likelihood refinement procedure implemented in *Refmac* (Murshudov *et al.*, 1996) using all data between 20.0 Å and the highest resolution, and manual model-building using *O* (Jones *et al.*, 1991). The R factor (R_{free}) after refinement is 21.3% (25.8%) for the monochromatic and 20.7% (26.8%) for the Laue data. The final model contains 252 waters for the monochromatic structure and 144 for the Laue structure, and the r.m.s. deviation for all Cα atoms between the two structures is 0.20 Å. Coordinates and structure factors for both the monochromatic and the Laue data have been deposited at the PDB.†

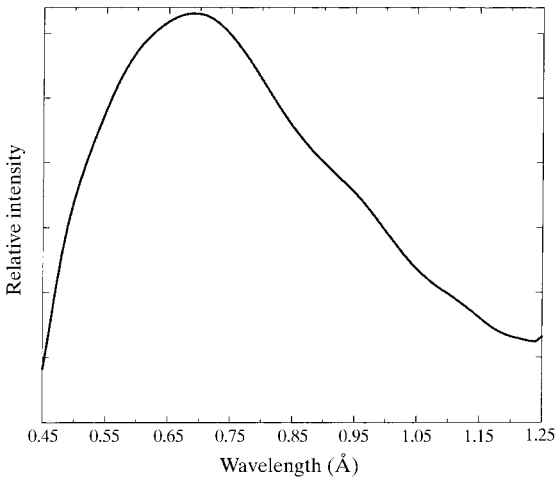

Fig. 3. Wavelength-normalization curve for ID9, ESRF, deduced from the Laue data set on AChE.

3. Discussion

Obtaining a data set of reasonable quality from Laue diffraction is not a guaranteed success for every crystallized protein. The Laue method has been applied with good results to well behaved proteins such as cutinase (Bourgeois *et al.*, 1997), restrictocin (Yang *et al.*, 1998) and photoactive yellow protein (Genick *et al.*, 1997), and to crystals of high symmetry, such as tomato bushy-stunt virus (Campbell *et al.*, 1990). Since the question of the exact pathway of reaction products from the active site of AChE has been raised, a suitable method has been searched for that would prove unequivocally whether or not there is a back door in the active-site gorge. Laue diffraction, with its extremely short exposure times and high information content per image, could very well supply this information, provided that four conditions are met:

(i) the initiation of the enzymatic reaction needs to be synchronized;

(ii) the reaction needs to be brought to a time scale commensurate with that of the data collection;

(iii) the existence of intermediate states needs to be ascertained and

(iv) the Laue data need to be of sufficient quality.

The synchronization is currently being investigated using caged compounds which have been developed for this purpose. The synthesis and chemical properties of nitrobenzyl derivatives of choline and of carbamylcholine have been studied, as well as their interaction with AChE, both in solution (Peng & Goeldner, 1996; Peng *et al.*, 1996) and in the crystal state using monochromatic crystallography (M. L. Raves, unpublished results). The temporal and spatial uniformity of reaction initiation depends on the penetration depth of the laser light into the crystal (Chen, 1994).

† Atomic coordinates and structure factors have been deposited with the Protein Data Bank, Brookhaven National Laboratory (References: 2ACK, R2ACKSF, 1AX9 and R1AX9SF).

Both the time scale of the release of choline from the active site and of the reaction of carbamylcholine are complex issues, since they must be measured in the crystal state, with hampered diffusion, at a temperature and pH that deviate from the conditions normally used for measuring the activity of the enzyme.

The existence of one intermediate state in the hydrolysis of ACh, the acetylated enzyme, is well known (Froede & Wilson, 1984). The carbamylated enzyme formed during the hydrolysis of carbamylcholine provides an even better intermediate that should be observable using time-resolved crystallography, because the decarbamylation of the enzyme is a much slower reaction than deacylation (Wilson *et al.*, 1960). However, since the pathway of the release of the reaction product of interest, choline, is unknown, the question whether a significantly populated intermediate state is involved in this release cannot be answered at this point.

The quality of the Laue data depends on the resolution and completeness attainable, the reliability of the measured intensities and the interpretability of the electron-density maps that follows from these factors.

3.1. *Quality of Laue data*

Unlike in monochromatic diffraction experiments, the high-resolution spots in a Laue image not only have a higher Bragg angle on average, placing them further towards the edge of the detector, but also result in a higher density of spots in all regions of the image. In the case of AChE, where all three unit-cell axes are longer than 100 Å and the mosaicity of the crystals is rarely below 0.2°, spatial overlap of spots is problematic. The resolution cut-off chosen for the data set described in the previous section, 2.8 Å, was based on the I/σ and completeness of the spots at higher resolution, and the conditions of the experiment. For the purpose of these studies and the kind of structural changes we hope to see, this resolution should be adequate.

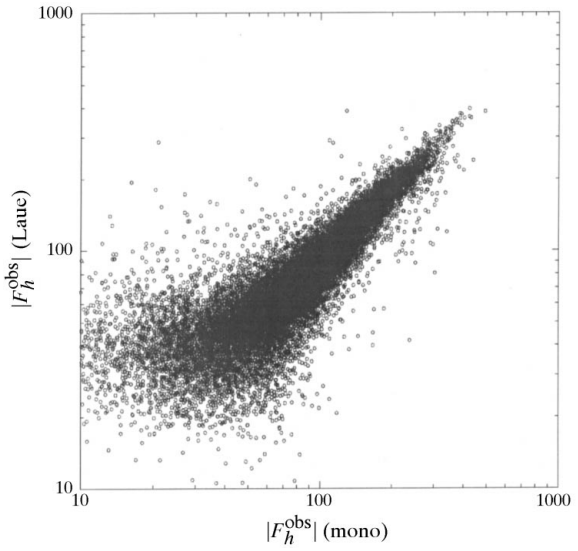

Fig. 4. Correlation plot between Laue and monochromatic structure-factor amplitudes. The correlation is 91.6%, based on 19725 unique reflections that were observed in both data sets.

In terms of completeness (see Table 2), the quality of the data set is very good: 95.2% in the medium-resolution range (5.6–3.4 Å). The problem of the low-resolution hole (Hajdu *et al.*, 1991) has largely been overcome, as judged by the completeness of 82.8% between ∞ and 5.6 Å ($2d_{min}$). High completeness at low resolution stems from the fact that a relatively large number (24) of frames were collected, aided by a powerful deconvolution algorithm (Ren & Moffat, 1995*b*). At higher resolutions, the completeness of the reflections is lower, but fully adequate for inclusion in the data set.

The amplitudes of the reflections correlate fairly well with those of the monochromatic data set. From Fig. 4 it can be seen that there is a slight tendency to overestimate weak reflections in the Laue data set, but the overall correlation coefficient of 91.6% indicates that the amplitudes are fairly reliable. The R_{sym} of the Laue data set (14.8 *versus* 6.5% for the monochromatic data up to 2.8 Å) also indicates a reduction in the quality of the data, but is still acceptable given the reduction in total X-ray exposure from several hours to 24 ms.

The problem of spatially overlapping spots, as observed in the data set, would have been aggravated by a substantial reduction of the crystal-to-detector distance (*e.g.* 200 instead of 300 mm). A reduction of the distance could improve the completeness and/or resolution limit of the data, as long as the software used for integration (Helliwell *et al.*, 1989; Ren & Moffat, 1995*a*; Bourgeois *et al.*, 1998) is capable of reliably deconvoluting most overlapping reflections. A θ offset of the detector, however, could have been instrumental in obtaining more unique data, as indicated by the Bragg cut-off in Fig. 2. Two data-collection strategies that could also have been beneficial for these crystals were described by Yang *et al.* (1998); regulation of the exposure time so as to reduce the extent of X-ray heating of the crystal, and utilization of two different exposure times to obtain well exposed low- and high-resolution data.

Since the program *LaueView* (Ren & Moffat, 1995*a*) gives the user full manual control of the integration, rejection and scaling criteria, the completeness of the data set is a trade-off against other parameters which are indicative for the quality of the data. For example, the inclusion of the non-redundant singles into the data set improved the completeness, but caused some deterioration in the correlation with the monochromatic data. In addition, the determination of the wavelength-normalization curve strongly depends on the accuracy of the intensities, and special care had to be taken not to include too many unreliable measurements, while still

being left with as high a redundancy as possible. The final wavelength-normalization curve obtained (Fig. 3) did not show fine details such as the Pt edges arising from the focusing mirror (Ren & Moffat, 1995*a*), but has the correct overall appearance.

3.2. *Map quality*

Special consideration was given to the problem of model bias in the initial electron-density maps, since the structure to be determined from the Laue data is very similar to that of the protein in the native state. To this effect, the same reflections that were used in the test set in the refinement of the initial starting model (Raves *et al.*, 1997) were flagged in the monochromatic and Laue data sets of the edrophonium complex (Kleywegt & Brünger, 1996). After rigid-body refinement of the entire protein, the difference between R and $R_{\rm free}$ indicates that most of the model bias has been avoided.

Fig. 5 shows a comparison of the Fourier difference maps after rigid-body refinement of the active-site region for the complete monochromatic data set (Fig. 5*a*), for the selection of reflections from the monochromatic data set which are present in the Laue data set (Fig. 5*b*) and for the Laue data set (Fig. 5*c*). As is to be expected, the electron-density difference maps made using the Laue data are of somewhat lower quality than the ones obtained using the monochromatic data; the signals are weaker, the maps are noisier and show less detail, which reflects the difference in $R_{\rm sym}$ values

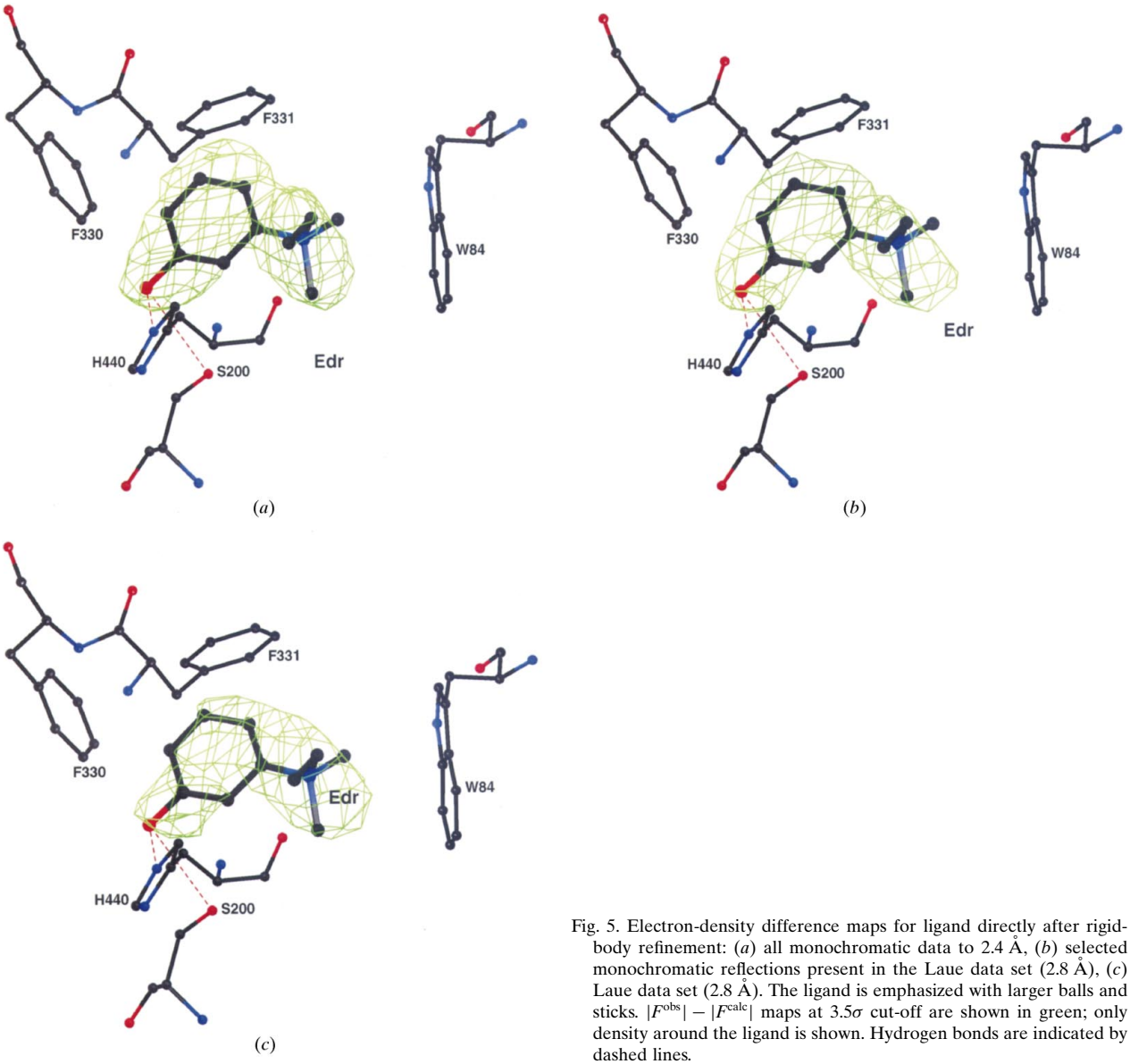

Fig. 5. Electron-density difference maps for ligand directly after rigid-body refinement: (*a*) all monochromatic data to 2.4 Å, (*b*) selected monochromatic reflections present in the Laue data set (2.8 Å), (*c*) Laue data set (2.8 Å). The ligand is emphasized with larger balls and sticks. $|F^{\rm obs}| - |F^{\rm calc}|$ maps at 3.5σ cut-off are shown in green; only density around the ligand is shown. Hydrogen bonds are indicated by dashed lines.

and completeness for the two data sets. Nevertheless, the difference map from the Laue data clearly shows the location, orientation and shape of the soaked-in inhibitor, edrophonium. In addition, a peak search on the initial Laue difference map yielded 78 peaks higher than 3.0σ that correspond to water molecules in the monochromatic structure, indicating that the maps are interpretable. For some of the incomplete side chains in the initial model (61 atoms in 23 different residues are disordered in the native structure), several atoms could be located in the maps for the monochromatic structure, reducing the number of missing atoms to 57 in 22 residues. The Laue maps showed even more of the missing atoms, leaving only 51 atoms in 19 residues undetermined. The amount of information that could be obtained from the Laue maps is somewhat surprising, given the quality of the data. It is especially encouraging to observe that the conformational change that O^{γ} of the active-site Ser200 undergoes upon binding of edrophonium (Harel *et al.*, 1993), from hydrogen bonding to His440 in the native state to interacting with the oxyanion hole in the complex, is visible in the electron-density maps of the Laue data set (see Fig. 6). Such detailed information will be extremely relevant in the determination of a transient intermediate structure and of structural changes during the enzymatic reaction.

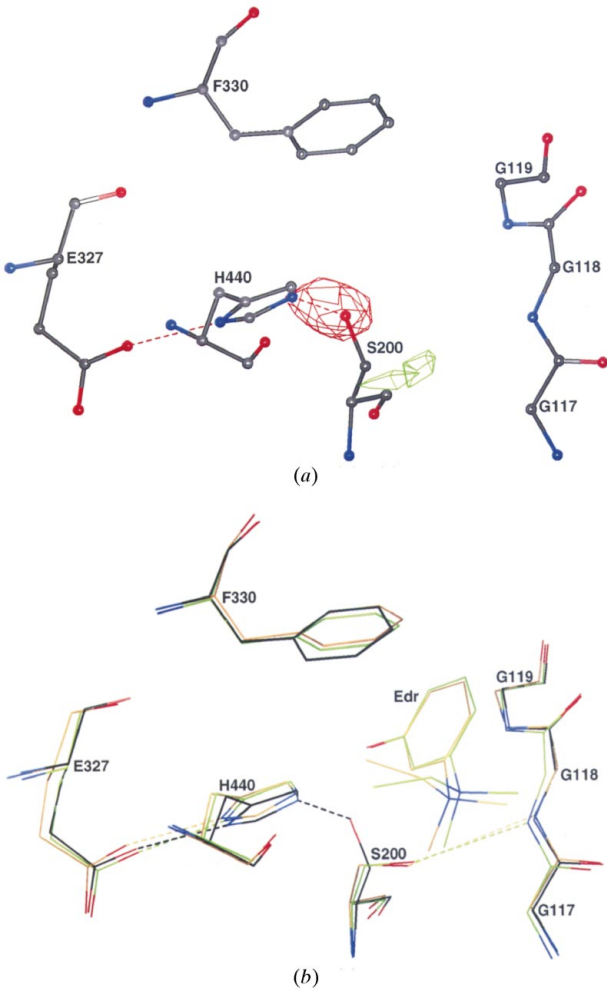

Fig. 6. Conformational change of Ser200 O^{γ} induced upon binding of the inhibitor edrophonium. (*a*) Electron-density difference maps from the Laue data directly after rigid-body refinement. $|F^{obs}| - |F^{calc}|$ maps, drawn in the vicinity of Ser200, are contoured at 2.7 and -2.7σ cut-off and shown in green and red, respectively. Protein residues in the native structure are shown in black. (*b*) Stick model of (i) the native starting model (shown in black), (ii) the refined model using monochromatic data (shown in green), (iii) the refined model using Laue data (shown in gold). Hydrogen bonds are indicated by dashed lines.

4. Conclusions

It has been shown that the Laue technique can be reliably applied to crystals of a protein as large as AChE in a static state. The maps from a data set of 24 images, with an overall completeness of 84.5% and an R_{sym} (unweighted) of 14.8%, clearly reveal the position of the ligand inside the active site and structural changes in important protein residues. The Laue data set does not represent the maximum quality attainable for AChE crystals: using a θ offset for the detector, two different exposure times and reducing the extent of X-ray heating of the crystal can improve the useful resolution limit and the reliability of the intensities. To improve the usefulness of the Laue method for AChE, future studies will concentrate on the synchronization of the initiation of the enzymatic reaction and its time scale.

This work was supported by the US Army Medical Research and Material Command under contract No. DADM17-93-C-3070, by the Kimmelman Center for Biomolecular Structure and Assembly, Rehovot, Israel, by Brookhaven National Laboratory and by the European Union. RBGR was supported by the Netherlands Foundation for Chemical Research (SON) with financial aid from the Netherlands Organization for Scientific Research (NWO). We thank K. Moffat for critical reading of the manuscript.

References

Axelsen, P. H., Harel, M., Silman, I. & Sussman, J. L. (1994). *Protein Sci.* **3**, 188–197.
Bolduc, J. M., Dyer, D. H., Scott, W. G., Singer, P., Sweet, R. M., Koshland, D. E. & Stoddard, B. L. (1995). *Science*, **268**, 1312–1318.
Bourgeois, D., Longhi, S., Wulff, M. & Cambillau, C. (1997). *J. Appl. Cryst.* **30**, 153–163.
Bourgeois, D., Nurrizo, D., Kahn, R. & Cambillau, C. (1998). *J. Appl. Cryst.* **31**, 22–35.
Bourne, Y., Taylor, P. & Marchot, P. (1995). *Cell*, **83**, 503–512.
Brünger, A.T., Kuriyan, J. & Karplus, M. (1987). *Science*, **235**, 458–460.

Campbell, J. W., Clifton, I. J., Greenhough, T. J., Hajdu, J., Harrison, S. C., Liddington, R. C. & Shrive, A. K. (1990). *J. Mol. Biol.* **214**, 627–632.
Chen, Y. (1994). PhD thesis, Cornell University.
Dougherty, D. A. (1996). *Science*, **271**, 163–168.
Faerman, C., Ripoll, D., Bon, S., Le Feuvre, Y., Morel, N., Massoulié, J., Sussman, J. L., & Silman, I. (1996). *FEBS Lett.* **386**, 65–71.
Froede, H. C. & Wilson, I. B. (1984). *J. Biol. Chem.* **259**, 11010–11013.
Genick, U. K., Borgstahl, G. E. O., Ng, K., Ren, Z., Pradervand, C., Burke, P. M., Šrajer, V., Teng, T.-Y., Schildkamp, W., McRee, D. E., Moffat, K. & Getzoff, E. D. (1997). *Science*, **275**, 1471–1475.
Gilson, M. K., Straatsma, T. P., McCammon, J. A., Ripoll, D. R., Faerman, C. H., Axelsen, P. H., Silman, I. & Sussman, J. L. (1994). *Science*, **263**, 1276–1278.
Grochulski, P., Li, Y., Schrag, J. D. & Cygler, M. (1994). *Protein Sci.* **3**, 82–91.
Hajdu, J., Almo, S. C., Farber, G. K., Prater, J. K., Petsko, G. A., Wakatsuki, S., Clifton, I. J. & Fülöp, V. (1991). *Crystallographic Computing* 5, edited by D. Moras, A. D. Podjarny & J.-C. Thierry, ch. 3, pp. 29–49. Oxford University Press.
Hammersley, A. P., Svensson, S. O. & Thompson, A. (1994). *Nucl. Instrum. Methods A*, **346**, 312–321.
Harel, M., Kleywegt, G. J., Ravelli, R. B. G., Silman, I. & Sussman, J. L. (1995). *Structure*, **3**, 1355–1366.
Harel, M., Schalk, I., Ehret-Sabatier, L., Bouet, F., Goeldner, M., Hirth, C., Axelsen, P. H., Silman, I. & Sussman, J. L. (1993). *Proc. Natl Acad. Sci. USA*, **90**, 9031–9035.
Helliwell, J. R., Habash, J., Cruickshank, D. W. J., Harding, M. M., Greenhough, T. J., Campbell, J. W., Clifton, I. J., Elder, M., Machin, P. A., Papiz, M. Z. & Zurek, S. (1989). *J. Appl. Cryst.* **22**, 483–497.
Jones, T. A., Zou, J. Y., Cowan, S. W. & Kjeldgaard, M. (1991). *Acta Cryst.* A**47**, 110–119.
Kleywegt, G. J. & Brünger, A. T. (1996). *Structure*, **4**, 897–904.
Kronman, C., Ordentlich, A., Barak, D., Velan, B. & Shafferman, A. (1994). *J. Biol. Chem.* **269**, 27819–27822.
Marchot, P., Khélif, A., Ji, Y. H., Mansuelle, P. & Bougis, P. E. (1993). *J. Biol. Chem.* **268**, 12458–12467.
Massoulié, J., Sussman, J. L., Bon, S. & Silman, I. (1993). *Prog. Brain Res.* **98**, 139–146.
Murshudov, G. N., Dodson, E. J. & Vagin, A. A. (1996). *Macromolecular Refinement: Proceedings of the CCP4 Study Weekend*, edited by E. Dodson, M. Moore, A. Ralph & S. Bailey, pp. 93–104. Warrington: Daresbury Laboratory.
Peng, L. & Goeldner, M. (1996). *J. Org. Chem.* **61**, 185–191.
Peng, L., Silman, I., Sussman, J. L. & Goeldner, M. (1996). *Biochemistry*, **35**, 10854–10861.
Quinn, D. M. (1987). *Chem. Rev.* **87**, 955–975.
Ravelli, R. B. G., Hezemans, A. M. F., Krabbendam, H. & Kroon, J. (1996). *J. Appl. Cryst.* **29**, 270–278.
Raves, M. L., Harel, M., Pang, Y.-P., Silman, I., Kozikowski, A. P. & Sussman, J. L. (1997). *Nature Struct. Biol.* **4**, 57–63.
Ren, Z. & Moffat, K. (1995*a*). *J. Appl. Cryst.* **28**, 461–481.
Ren, Z. & Moffat, K. (1995*b*). *J. Appl. Cryst.* **28**, 482–493.
Ripoll, D. R., Faerman, C. H., Axelsen, P. H., Silman, I. & Sussman, J. L. (1993). *Proc. Natl Acad. Sci. USA*, **90**, 5128–5132.
Schlichting, I., Almo, S. C., Rapp, G., Wilson, K., Petratos, K., Lentfer, A., Wittinghofer, A., Kabsch, W., Pai, E. F., Petsko, G. A. & Goody, R. S. (1990). *Nature (London)*, **345**, 309–315.
Šrajer, V., Teng, T., Ursby, T., Pradervand, C., Ren, Z., Adachi, S., Schildkamp, W., Bourgeois, D., Wulff, M. & Moffat, K. (1996). *Science*, **274**, 1726–1729.
Sussman, J. L., Harel, M., Frolow, F., Oefner, C., Goldman, A., Toker, L. & Silman, I. (1991). *Science*, **253**, 872–879.
Tan, R. C., Truong, T. N., McCammon, J. A. & Sussman, J. L. (1993). *Biochemistry*, **32**, 401–403.
Verdonk, M. L., Boks, G., Kooijman, H., Kanters, J. A. & Kroon, J. (1993). *J. Comput. Aided Mol. Design*, **7**, 173–182.
Wilson, I. B., Hatch, M. A. & Ginsburg, S. (1960). *J. Biol. Chem.* **235**, 2312–2315.
Yang, X., Ren, Z. & Moffat, K. (1998). *Acta Cryst.* D**54**, 367–377.